ice
Institution of Civil Engineers
Publishing

ICE Handbook of Geosynthetic Engineering

Geosynthetics and their applications

Third edition

Edited by
Sanjay Kumar Shukla

Figure 1.29 Laboratory tests related to geosynthetic survivability and the separation function. (Reproduced from Hausmann (1990), The McGraw-Hill Companies)

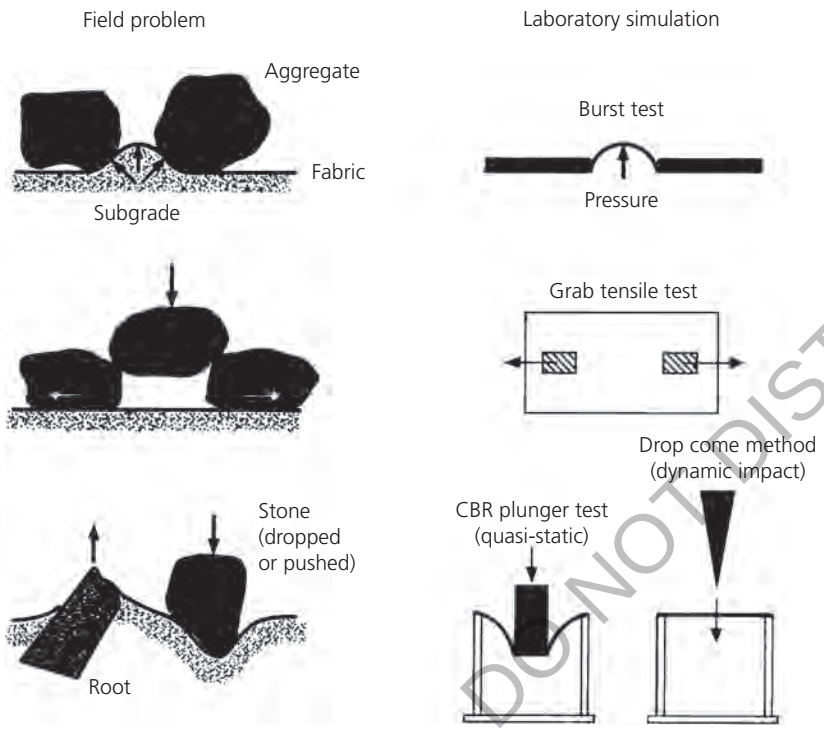

Figure 1.30 Comparison of pull-out and direct shear tests with corresponding reinforcing application. (Reproduced from Paulson (1987), with permission from Elsevier)

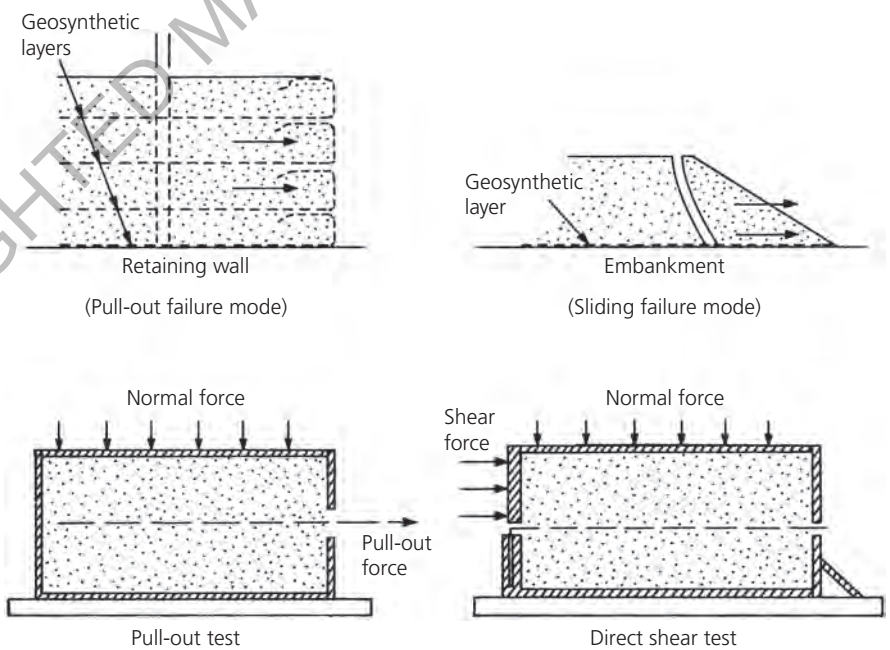

Figure 4.4 External stability checks: (a) sliding, (b) overturning, (c) bearing capacity and (d) deep-turning stability

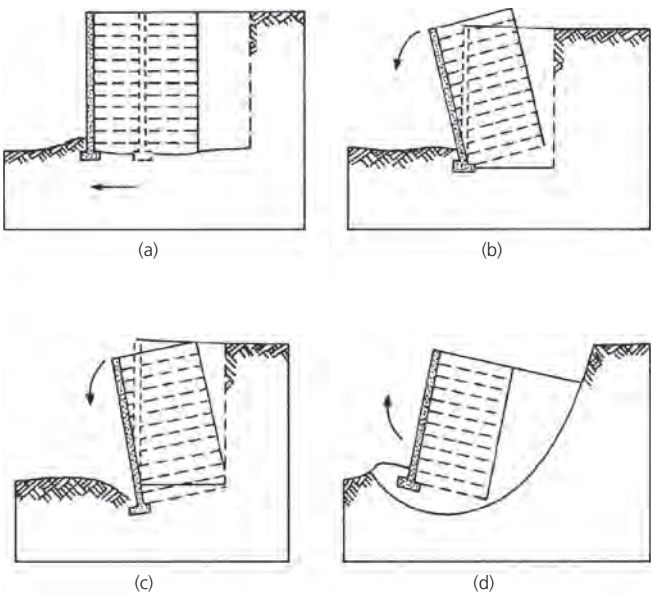

Figure 4.5 Analysis of a reinforced earth-retaining wall

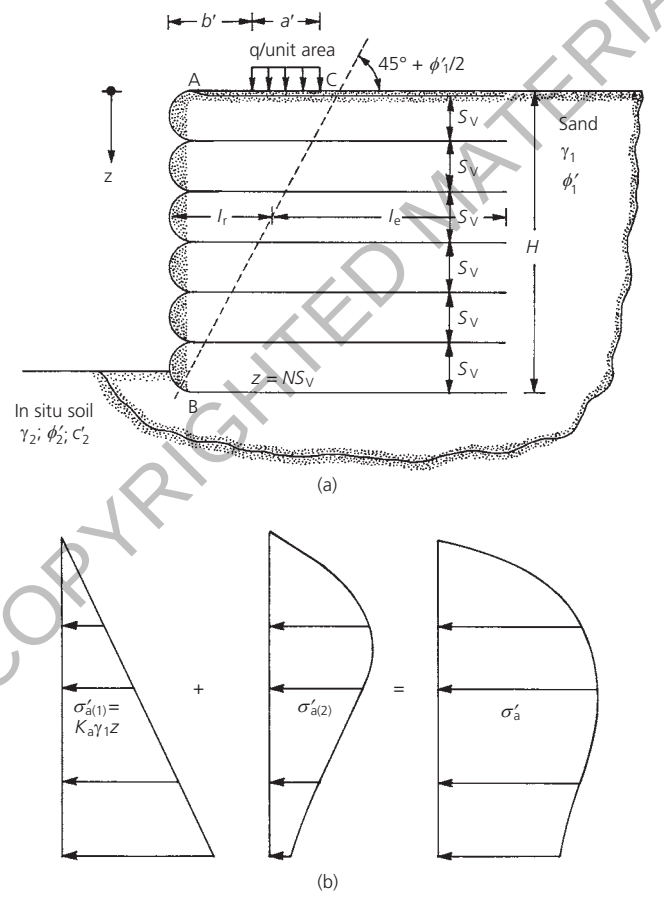

backfill, the in situ soil has a unit weight of γ_2, an effective friction angle of ϕ'_2 and a cohesion of c'_2. A surcharge with an intensity of q per unit area lies at the top of the retaining wall. The wall has geosynthetic reinforcement ties at depths $z = 0$, S_V, $2S_V$, …, NS_V. The height of the wall is $NS_V = H$.

According to the Rankine active earth pressure theory

$$\sigma'_a = \sigma'_v K_a - 2c' \sqrt{K_a} \tag{4.1}$$

Where σ'_a is the Rankine active earth pressure at any depth z.

For dry granular soils with no surcharge at the top, $c' = 0$, $\sigma'_v = \gamma_1 z$ and $K_a = \tan^2(45 - \phi'_1/2)$. Thus

$$\sigma'_{a(1)} = \gamma_1 z K_a \tag{4.2}$$

When a surcharge is added at the top, as shown in Figure 4.5(a), then

$$\begin{aligned} \sigma'_v &= \sigma'_{v(1)} + \sigma'_{v(2)} \\ &= \gamma_1 z \overbrace{\text{due to soil only}} \quad \overbrace{\text{due to the surcharge}} \end{aligned} \tag{4.3}$$

The magnitude of $\sigma'_{v(2)}$ can be calculated by using the 2:1 method of stress distribution, and is shown in Figure 4.6(a). According to Laba and Kennedy (1986)

$$\sigma'_{v(2)} = \frac{qa'}{a' + z} \quad (\text{for } z \le 2b') \tag{4.4}$$

and

$$\sigma'_{v(2)} = \frac{qa'}{a' + \frac{z}{2} + b'} \quad (\text{for } z > 2b') \tag{4.5}$$

Also, when a surcharge is added at the top, the lateral pressure at any depth is

$$\begin{aligned} \sigma'_a &= \sigma'_{a(1)} + \sigma'_{a(2)} \\ &= K_a \gamma_1 z \overbrace{\text{due to soil only}} \quad \overbrace{\text{due to the surcharge}} \end{aligned} \tag{4.6}$$

According to Laba and Kennedy (1986), $\sigma'_{a(2)}$ may be expressed as (Figure 4.6(b))

$$\sigma'_{a(2)} = M\left(\frac{2q}{\pi}(\beta - \sin\beta\cos 2\alpha)\right) \quad \overbrace{\text{in radians}} \tag{4.7}$$

where

$$M = 1.4 - \frac{0.4b'}{0.14H} \ge 1 \tag{4.8}$$

The geomembrane should be placed when most of the anticipated differential settlements have occurred. To determine the right time for this action, the deformation of the interim cover surface should be monitored.

14.8.2 Regulating the soil and gas-venting layer

Solid wastes are not suitable for finish profiling; a regulating soil layer is required for this purpose. If gas is generated in the landfill body, a gas-venting system has to be installed below the cover. The functions of the regulating layer and the gas-venting layer may be combined by using sufficiently pervious soil. Geosynthetic drainage composites may be used as gas collectors if the permeability of the regulating soil layer cannot be relied upon. The collected gas has to be conducted out of the landfill by pipes and shafts, and should be processed for energy use, or it has to be burnt. Figure 14.8 shows a shaft for the collection of gas in the cover system.

14.8.3 Mineral sealing layer

For covers on deposits of inert mineral residues, and for interim sealing layers of municipal waste landfills, a compacted clay layer placed in two lifts, each 0.25 m thick with a hydraulic conductivity of no more than 5×10^{-9} m/s, is used.

Figure 14.8 Gas shaft in a cover system of a landfill. (Courtesy of SKZ – Testing)

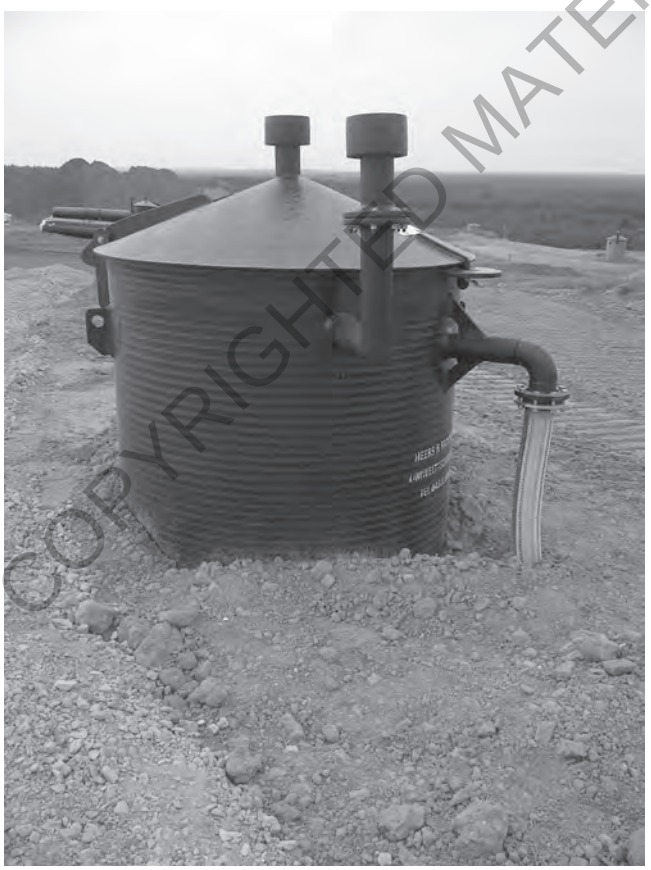

Mineral liners in capping systems are exposed to fluctuations in their water content. Under central European climatic conditions, the evapotranspiration rate is relatively high during the growing season, from about April until late September, while at the same time precipitation may be low. During this period, the water content of the clay layer is reduced. In autumn and winter, evapotranspiration is decreasing, precipitation may be high and the mineral liner is rewetted. Observations by Melchior (1993) at large test fields indicate that, under certain unfavourable boundary conditions, desiccation causes the formation of micro-fissures and cracks in the cohesive cover soil during summer. These defects do not heal, and are utilised by plants for root paths. The detrimental effect of the desiccation due to thermal gradients is increased further by the suction of the roots. As a result, within two to three climatic cycles, the mineral liner experiences fissuring to a considerable extent, the overall hydraulic conductivity increases and the sealing function is impeded.

14.8.4 GCLs in cover systems

Today, mainly GCLs are installed. The question of the equivalency of GCLs and CCLs has been discussed by Koerner and Daniel (1995) and Stief (1995), among others. The properties, testing methods and quality assurance aspects of GCLs have been compiled by Gartung and Zanzinger (1998). Fox and Stark (2015) and Stark and Newman (2015) analysed the stability of GCLs in the interface to other geosynthetics or soils in a cover lining system. Zanzinger (2016) investigated the long-term internal shear strength of GCLs.

Practical experience shows that GCLs, as part of a capping system, have some advantages over CCLs. Handling and installation are much easier, less time is needed for placement, waste storage space can be saved due to the lesser thickness, and the quality of the manufactured geosynthetic product shows less variability than that of natural clay soils.

On the other hand, it has to be kept in mind that, due to the low thickness and mass of bentonite, GCLs are extremely sensitive to damage during and after construction, and thus great care must be taken in construction when using GCLs. The design of a geosynthetic barrier containing GCLs must ensure that desiccation of the GCLs is avoided, for a number of reasons. For example, dried-out sodium bentonite will exchange cations with the adjacent soil and become calcium bentonite, which has much poorer swelling properties than sodium bentonite. In some projects in Germany, it was found that, under certain conditions and with inadequate protection of the GCLs against desiccation, the barrier function of the GCLs was lost (Zanzinger and Touze-Foltz, 2009).

The chemical composition and thickness of cover materials must be considered during the design phase, as these factors can impact on the performance of the GCL. Buckley *et al.* (2010) have shown that the cover material can have a marked influence on the performance of a GCL used in a capping liner. They suggested some measures to limit the detrimental effects of

Figure 16.9 The Mulhouse Canal (France) – extruded concrete sliding formwork machine. (Courtesy of D. Croissant, Cemagref (1997))

the experimental basin of the INRAE site in Aix-en-Provence (Martinot *et al.*, 2022). Three questions of particular interest were investigated.

- What is the minimum (heating) power for optimum leak detection?
- What is the minimum leakage rate detectable for the minimum heating energy? This question is closely linked, on the one hand, to the detection criterion, that is a temperature difference, which can only be explained by the presence of an anomaly (i.e. a leak), and, on the other hand, to the distance of the leak relative to the positioning of the optical fibre.
- Is the system as efficient in hot periods (summer) as in cold periods (winter)?

INRAE's experimental basin is located in the vicinity of Aix-en-Provence. The surface area of the basin is 200 m^2, while the volume of water retained is 210 m^3 (Figure 16.10). The basin has a 2.5 m-high embankment; the slopes are 2H:1V on the inside of the basin, and 3H:2V on the outside. The embankment is made of a local silty clay with a plasticity index of 17 and a hydraulic conductivity of 10^{-9} m/s.

Figure 16.10 A view of INRAE's experimental field site. (Courtesy of INRAE (personal communication, 2019))

A geomembrane lining system was placed on the inside of the basin. One part was a Draintube drainage geocomposite made up of mini-drains 20 mm in diameter spaced 2 m apart (Figure 16.11). The drainage geocomposite was installed directly on the soil. The mini-drains followed the slope, and were connected to a central drain, filled with gravel. This drain evacuates water through a pipe crossing the embankment. The second part of the lining system was a 1 mm thick PP geomembrane placed above the geocomposite. Fourteen artificial leaks crossed the geomembrane, and found outlets in the drainage geocomposite (see Figure 16.11). These leaks were used during the experiment described. The leaks simulated geomembrane damage, in order to study the influence of exposure to the sun (the effect of temperature), and how their position affected the efficiency of leak detection compared with that of the mini-drains. Each leak was connected to the water supply with a garden hose.

Part of the monitoring system consisted of an optical fibre associated with a copper cable, together called an active fibre, placed in contact with the soil at the embankment toe. Additional sensors were used to confirm the fibre-optic measurements: humidity sensors and water content sensors located downstream of the leaks. Temperature sensors measured the temperature of the water, both in the basin and at the leaks. Water from the basin directly supplied the leaks, using pumps, so that the temperatures were close to each other. The flow rate and water pressure were controlled through a valve upstream of the leaks, and recorded during the experiments.

A Sensornet Oryx interrogator was used to measure the temperature along the optical fibre. A spatial resolution of 1 m was selected, and an acquisition frequency of 5 min. The electrical power injected during the heating operations (voltage and intensity) was recorded by means of a recording power meter

material, typically a geonet, installed over the substrate and fastened by means of impact anchors (Figure 18.10). The geonet is covered by the waterproofing composite geomembrane. The drainage system provided behind the composite geomembrane collects the water and discharges it outside the tunnel when possible; if outside discharge is not possible, patented one-way valves, made of the same composite geomembrane material, operated by pressure differentials and discharging inside the tunnel, are available. The relief valves will open only when the pressure inside the tunnel is less than the pressure from the surrounding soil, usually when the tunnel is empty. The valves discharge inside the tunnel the water conveyed by the drainage layer. Other types of geosynthetics are also used as drainage in underground applications as described by Cazzuffi *et al.* (1986).

18.3.3 Waterproofing liner

The waterproofing layer used in the state-of-the-art projects is a very low-permeability composite geomembrane, composed of a PVC geomembrane, a few millimetres thick, bonded during fabrication to a geotextile that enhances its anti-puncture resistance, placed over the substrate/support/drainage layers (Figure 18.11).

Figure 18.10 A geonet fastened to the substrate by means of impact nails

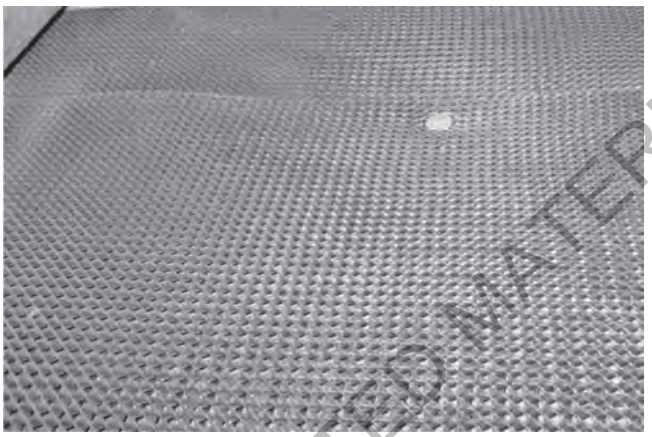

Figure 18.11 Placing of the composite geomembrane inside a pressure tunnel in the Czech Republic

Particular provisions, such as an additional layer of geotextile, must be made to avoid the intrusion of the waterproofing liner into possible cracks in the substrate, in presence of high-water heads. The composite geomembrane is left exposed to contact with the water flowing inside the tunnel, and is designed to withstand mechanical actions (abrasion, impact and tear) due to flowing water (Figures 18.12 and 18.13), and transported materials and sediments.

18.3.4 Fastening system

The fastening system consists of lines of stainless-steel profiles, anchoring the composite geomembrane to the substrate, be it

Figure 18.12 Exposed composite geomembrane in a free-flow tunnel

Fig. 18.13 Exposed composite geomembranes to resist high water velocities and turbulence